

Copolymers of Thiophene and Thiazole. Regioregulation in Synthesis, Stacking Structure, and Optical Properties

Takakazu Yamamoto,* Minoru Arai, and Hisashi Kokubo

Chemical Resources Laboratory, Tokyo Institute of Technology, 4259 Nagatsuta, Midori-ku, Yokohama 226-8503, Japan

Shintaro Sasaki

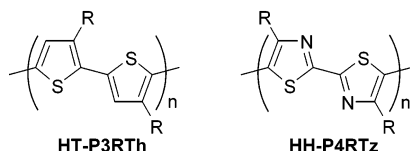
Japan Advanced Institute of Science and Technology, 1-1 Asahidai, Tatsunokuchi, Ishikawa 923-1211, Japan

Received March 11, 2003; Revised Manuscript Received August 2, 2003

ABSTRACT: Palladium-catalyzed polycondensation between 2,5-dibromo-4-alkylthiazoles (alkyl = butyl thorough nonyl) and 2,5-bis(trimethylstannyl)thiophene gave charge-transferred-type alternating polymers, PTz(R)Th's. PTz(R)Th's had a high regioregularity as judged from their ^1H NMR and X-ray diffraction (XRD) data, and the head-to-tail content was estimated to be higher than 90% from the ^1H NMR data. The polymer forms a stacked structure, and the stacked structure is proposed based on the XRD data. The tendency of the polymer to form the stacked structure is considered to contribute to the regioregulation in the polymerization. The polymer was susceptible to both electrochemical oxidation (or p-doping) and reduction (or n-doping).

Introduction

Stacking of π -conjugated polymers is currently the subject of intense study.^{1–9} Regioregular poly(3-alkylthiophene-2,5-diyl)^{1,2} (e.g., head-to-tail-type HT-P3RTh)-prepared by McCullough¹ and Rieke² and poly(4-



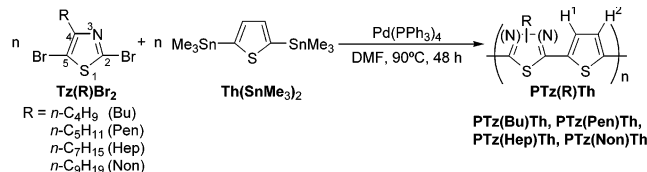
alkylthiazole-2,5-diyl)^{5c–e,7a} (e.g., head-to-head-type HH-P4RTz) constituted of recurring five-membered heteroaromatic rings easily form such a stacked solid structure. The polymer structure constituted of the recurring five-membered rings seems to be suited for forming the π -stacked structure.¹⁰

On the other hand, it has been reported that π -conjugated polymers with a charge-transferred (CT) structure along the polymer main chain show interesting electrochemical, optical, and electronic properties,^{11–15} including their large optical third-order nonlinear susceptibility, $\chi^{(3)}$.

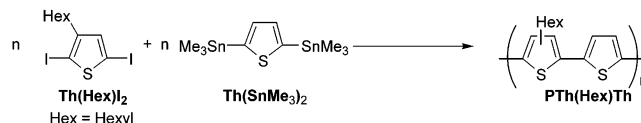
However, these chemical and physical properties have been studied mainly with CT-type copolymers constituted of electron-donating five-membered heteroaromatic rings (e.g., thiophene) and electron-accepting six-membered heteroaromatic rings (e.g., pyridine),¹¹ and the stacking behavior of CT-type copolymers constituted of electron-donating five-membered aromatic rings and electron-accepting five-membered aromatic rings has received less attention. Preparation of a five-membered-ring CT-type copolymer with alternating 3,4-dinitrothiophene and 3,4-aminothiophene units has been reported by Zhang and Tour.¹⁴ However, this copolymer does not seem to form the stacked structure due to the presence of rather bulky nitro and amino substituents at all the 3,4-positions of the thiophene rings.

We now report that the following CT-type copolymer between electron-accepting thiazole^{5c–e,7a} and electron-

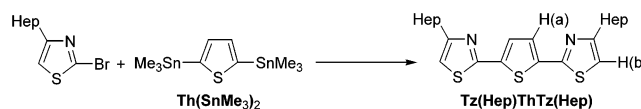
Scheme 1



Scheme 2



Scheme 3



donating thiophene shows a strong tendency to stack, forming a new type of packing structure in the solid (Scheme 1).

For comparison, a copolymer between 3-alkylthiophene and thiophene (Scheme 2) and a trimeric model compound (Scheme 3) were prepared analogously.

Experimental Section

Monomers. Tz(R)Br₂'s shown in Scheme 1 were prepared through 2-amino-4-alkylthiazoles^{5c,16} in ways analogous to those previously reported^{5c} and were characterized by ^1H NMR, IR, and data from elemental analysis. For example, the data for Tz(Hep)Br₂ are as follows. ^1H NMR (CDCl₃): δ , 2.72 (t, 7.9 Hz, 2H), 1–1.8 (m, 10H), 0.86 (t, 3H). Anal. Calcd for C₁₀H₁₅Br₂NS: C, 35.21%; H, 4.43%; N, 4.11%. Found: C, 35.00%; H, 4.29%; N, 3.99%.

Polymerization. PTz(R)Th's and PTh(Hex)Th were prepared in manners similar to those previously reported,^{5b,c} which used the corresponding dihalo-monomer, 2,5-bis(trimethylstannyl)thiophene, and Pd(PPh₃)₄¹⁷ catalyst (cf. Scheme 1), and were mainly characterized by ^1H NMR. For example,

Table 1. CV and Optical Data of PTz(R)Th

no.	polymer	CV, ^a V vs Ag ⁺ /Ag				UV-vis, λ_{max} , nm			
		p-doping (x)	p-dedoping	n-doping (x)	n-dedoping	in TFA ^b ($\epsilon/10^4 \text{ M}^{-1} \text{ cm}^{-1}$)	film ^c	PL, ^d nm	IP, ^e eV
1	PTz(Bu)Th	0.66 (0.050)	0.43	-2.11 (0.30)	-1.93	466 (1.94)	483, 529, 575	592	
2	PTz(Pen)Th	0.68 (0.048)	0.54	-2.05 (0.25)	-1.99	467 (1.93)	507, 541, 590	601	5.24
3	PTz(Hep)Th	0.70 (0.046)	0.49	-2.09 (0.16)	-1.93	463 (1.97)	504, 534, 592	593	
4	PTz(Non)Th	0.74 (0.053)	0.53	-2.15 (0.18)	-1.93	467 (2.40)	520, 560, 605	594	5.41

^a Data of cyclic voltammetry. Measured with a cast film on a Pt electrode. x = doping level (charge stored per the repeating unit).

^b TFA = trifluoroacetic acid. ^c With a cast film on a quartz glass plate. ^d Photoluminescence peak measured in TFA. ^e IP = ionization potential.

the data for PTz(Hep)Th are as follows. ¹H NMR (CF₃COOD): δ , 8.19 (1H), 7.65 (1H), 3.23 (2H), 1.92 (2H), 1.2–1.7 (8H), 0.92 (3H). Anal. Calcd for (C₁₄H₁₇NS₂·0.2H₂O)_{*n*}: C, 62.93%; H, 6.57%; N, 5.25%; S, 24.01%. Found: C, 62.52%; H, 6.40%; N, 5.18%; S, 23.23%. $[\eta]$ (CF₃COOH, 30 °C) = 0.40 dL g⁻¹. Yield = 86%. The yields of PTz(Bu)Th, PTz(Pen)Th, and PTz(Non)Th were 90, 73, and 87%, respectively. ¹H NMR data of other polymers are described in the text.

Synthesis of the Trimer Tz(Hep)ThTz(Hep). An anhydrous dimethylformamide (DMF) (30 mL) solution containing 2-bromo-4-heptylthiazole^{5c,16} (204 mg, 0.78 mmol), Pd(PPh₃)₄,¹⁷ and 2,5-bis(trimethylstannyl) thiophene (159 mg, 0.39 mmol) in a Schlenk tube was stirred at 90 °C for 24 h under reflux. The reaction mixture was poured into an aqueous solution of potassium fluoride. The product was extracted with chloroform and dried with Na₂SO₄. After condensation with an evaporator, the crude product was obtained by column chromatography on SiO₂ (eluent = 1:1 mixture of chloroform and hexane; R_f = 0.55). The product was purified by high-performance liquid chromatography (HPLC). Yield = 79 mg (45%; yellow oil). ¹H NMR (CDCl₃, 400 MHz): δ , 7.43 (s, 2H, H(a) in Scheme 3), 6.53 (s, 2H, H(b)), 2.78 (t, 7.8 Hz, 4H), 1.2–1.8 (m, 20H), 0.89 (t, 7.3 Hz, 6H). ¹³C{¹H} NMR (CDCl₃, 100 MHz): δ , 160.2, 158.9, 126.3, 112.5, 31.8, 31.6, 29.3, 29.1, 22.7, 14.1.

Measurements. ¹H NMR spectra, UV-vis spectra, and photoluminescence spectra were recorded on a JEOL JNM-EX 400 spectrometer, a Shimadzu UV-3100PC spectrometer, and a Hitachi F-4010 spectrometer, respectively. Thin films of PTz(R)Th on a quartz glass plate were prepared by casting from CF₃COOH solutions of the polymers and drying under a vacuum. The film was further treated with aqueous ammonia and dried under a vacuum when necessitated. Cyclic voltammograms (CVs) were taken using Hokuto Denko HA-501 galvanostat/potentiostat and a Hokuto Denko KB-104 function generator. A CF₃COOH solution of PTz(R)Th was cast on a Pt plate (1 cm × 1 cm) and dried under a vacuum. The film thus obtained was dipped in diluted ammonia and dried under a vacuum for the CV measurement. Powder X-ray diffraction (XRD) data were obtained with a Philips PS-1051 instrument. Viscosity was measured with an Ubbelohde viscometer. Gel permeation chromatography (GPC) analysis was carried out with a Shimadzu HIC-6A chromatograph using chloroform as the eluent and polystyrene standards. The density of the polymer was measured by a sink and float test using aqueous solutions of ZnCl₂. Repeated measurements of the density indicated that the measurement had the accuracy of about 0.02 g cm⁻³. Ionization potentials of PTz(Non)Th and PTz(Pen)Th were kindly measured at Mitsubishi Chemical Corp. by using an AC-1 apparatus purchased from RIKEN KEIKI Co. Ltd.

Results and Discussion

Synthesis of Polymers. The polycondensation expressed by Scheme 1 proceeded well to give PTz(R)Th in 73–90% yield. IR and ¹H NMR spectra were reasonable, and the peaks originated from the -SnMe₃ groups were not observed in the spectra. PTz(R)Th was soluble in CF₃COOH and concentrated H₂SO₄. However, its solubility in common organic solvents was low; it was partially (about half) soluble in chloroform. GPC analysis of the chloroform-soluble part of PTz(Non)Th gave

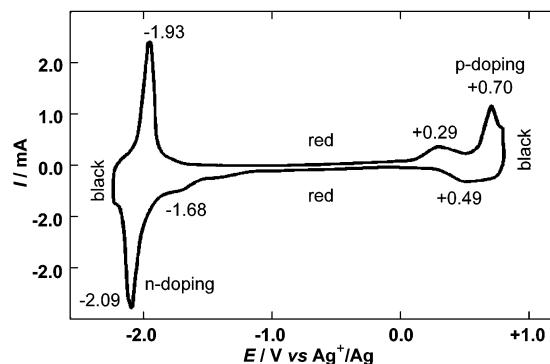


Figure 1. Cyclic voltammogram of a film of PTz(Non)Th on a Pt plate, in an acetonitrile solution of 0.10 M [NEt₄]BF₄ at room temperature. Scan rate = 100 mV s⁻¹.

the number-average molecular weight (M_n) of 2200 and weight-average molecular weight (M_w) of 2650.¹⁸ The remaining chloroform-insoluble part is considered to have a higher molecular weight. Casting from a CF₃COOH solution of the polymer on substrates (e.g., on a quartz glass plate), treating the film with aqueous ammonia, and drying under a vacuum gave a solvent-free film which was of good quality and was suited for electrochemical and optical measurements. PTz(Bu)Th, PTz(Pen)Th, PTz(Hep)Th, and PTz(Non)Th gave intrinsic viscosities of 0.30, 0.46, 0.40, and 0.85 dL g⁻¹ in CF₃COOH at 30 °C, respectively. They showed 5 wt % loss temperatures at 409, 428, 437, and 289 °C, respectively. The polymers were stable under air at room temperature and gave the same IR spectra after leaving them for 4 years.

CVs (e.g., Figure 1) of their cast films on a Pt plate exhibited a main oxidation (or p-doping) peak at 0.70 ± 0.04 V versus Ag⁺/Ag and a reduction (or n-doping) peak at -2.10 ± 0.05 V versus Ag⁺/Ag in a CH₃CN solution of 0.10 M [NEt₄]BF₄, and the peaks were coupled with p-dedoping and n-dedoping peaks at 0.49 ± 0.05 V and -1.93 V versus Ag⁺/Ag, respectively. These results support the structure of the polymer having both the electron-donating thiophene unit and the electron-accepting thiazole unit; CT-type polymers are usually susceptible to both p-doping and n-doping.^{11,12} According to the electrochemical reaction, the polymer film changes its color (electrochromism) as shown in Figure 1. Table 1 summarizes the CV data and optical data of the polymers. The n-doping peak was larger than the p-doping peak, since p-doping proceeds only with the thiophene unit and n-doping can proceed not only in the thiazole^{5c} unit but also in the thiophene^{19a} unit. Polythiophene usually undergoes p-doping,^{1e,19b-d} however, it also can accept electrons to generate an n-doped state.^{19a} The red film of PTz(R)Th turned black after p-doping and n-doping; the color returned to red

Chart 1. Triads in the Copolymer

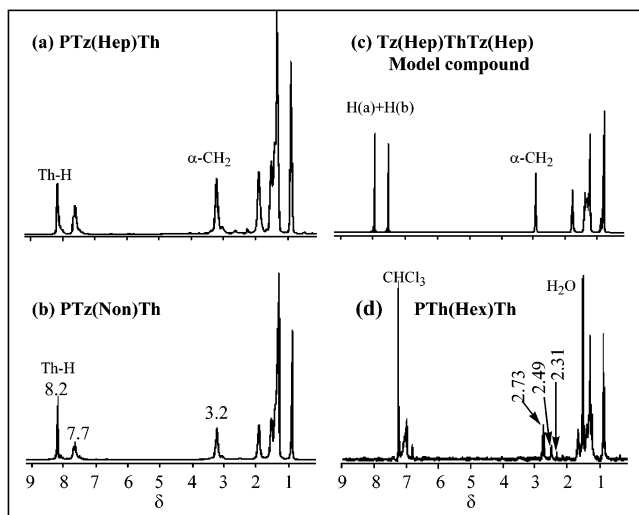
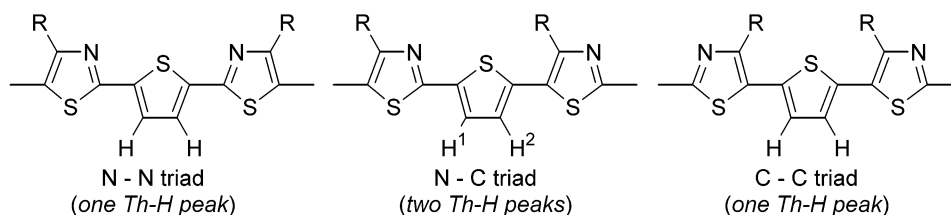


Figure 2. ^1H NMR of (a) PTz(Hep)Th in CF_3COOD , (b) PTz(Non)Th in CF_3COOD , (c) Tz(Hep)ThTz(Hep) in CF_3COOD , and (d) PTh(Hex)Th in CDCl_3 . The ^1H NMR spectra of PTz-(Bu)Tz and PTz(Pen)Tz gave the $\alpha\text{-CH}_2$ signal similar to that of PTz(Non)Tz, which shows one main peak in the $\alpha\text{-CH}_2$ region. The solubility of PTh(Hex)Th in CDCl_3 was lower than that of PTz(R)Th in CF_3COOD .

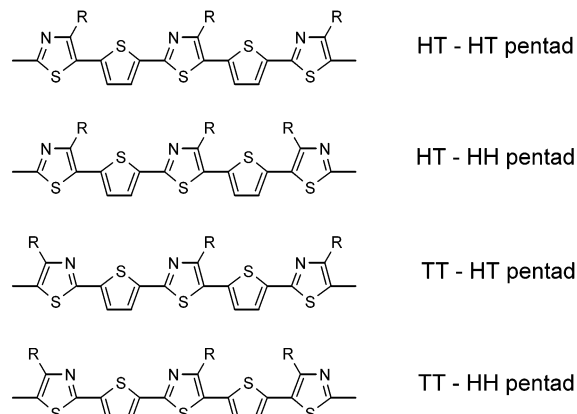
after dedoping. It is interesting that the first p-doping oxidation wave does not have its partner reduction wave until -1.68 V. Similar behavior has been observed with CT-type π -conjugated polymers (e.g., copolymers between electron-accepting pyridine and electron-donating thiophene^{11a,b}) and been assigned to occurrence of a stabilization reaction after the electrochemical reaction. From a potential difference between the onset of the p-doping and that of the main n-doping peak at -2.09 V (cf. Figure 1), the band gap of PTz(Non)Th is estimated at about 2.0 eV, which agrees with the band gap estimated from the onset position of the UV-vis absorption band of PTz(Non)Th (1.8–2.0 eV).

PTz(Non)Th and PTz(Pen)Th showed an ionization potential of 5.3 ± 0.1 eV, respectively, and from this ionization potential and the band gap the electron affinity of the polymer was estimated at about 3.3 eV.

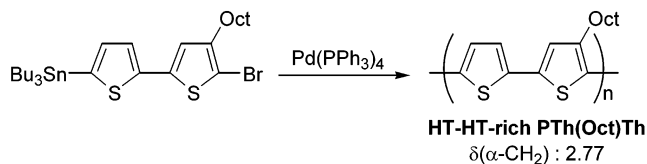
Figure 2 exhibits the ^1H NMR spectra of (a) PTz(Hep)Th, (b) PTz(Non)Th, (c) the model compound Tz(Hep)ThTz(Hep), and (d) PTh(Hex)Th. As depicted in Scheme 1, if PTz(R)Th has a random copolymer structure, PTz(R)Th has two kinds of bonds between the thiazole and thiophene units, and H^1 and H^2 protons of thiophene have magnetic circumstances in the triadlike expression as shown in Chart 1.

The model compound Tz(Hep)ThTz(Hep) corresponds to the N–N triad, and its ^1H NMR spectrum gives only one Th–H peak and one $\alpha\text{-CH}_2$ peak of the R group, respectively. If PTz(R)Th has the random copolymer structure as described above, it may give a complex peak pattern for the Th–H protons (e.g., one peak for the N–N triad, one pair of peaks for the N–C triad, and

Chart 2. Pentads in the Copolymer



Scheme 4

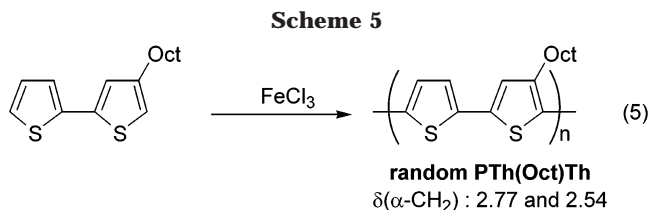


one peak for the C–C triad as shown in Chart 1). However, PTz(R)Th gives rise to essentially only two peaks as shown in Figure 2, suggesting formation of a controlled structure (presumably a head-to-tail-type regioregular structure consisting of the N–C triad). Of the two peaks at $\delta 8.2$ and 7.7 , the somewhat broadened peak at $\delta 7.7$ may be assigned to the H^2 proton in the N–C triad in Chart 1, and this broadening may originate from coupling with the CH_2 protons in R.

In a pentad expression, the $\alpha\text{-CH}_2$ protons of the R group have the circumstances shown in Chart 2, similar to cases of poly(3-alkylthiophene-2,5-diyl), P3RTh.^{1–5}

However, appearance of one strong $\alpha\text{-CH}_2$ peak at $\delta 3.2$ and only minor peak(s) in a range of $\delta 2\text{--}3$ in Figure 2a,b suggests that certain selection of the bond formation takes place during the polymerization, which gives a precipitated crystalline (vide infra) solid of the polymer, to yield one of the pentads (presumably the HT-HT pentad) selectively. To the contrary, in the case of copolymerization between 3-hexylthiophene and thiophene (cf. Scheme 2), such selection does not seem to take place, since the obtained copolymer shows several $\alpha\text{-CH}_2$ peaks of the hexyl group in a range $\delta 2\text{--}3$ in Figure 2d. Recently, Moreau^{20a} reported that regioregular HT-HT pentad-rich PTh(Oct)Th (Oct = octyl) prepared according to the polycondensation in Scheme 4 shows an $\alpha\text{-CH}_2$ main peak at $\delta 2.77$ whereas regiorregular PTh(Oct)Th prepared by oxidative polymerization of octylbithiophene (Scheme 5) shows two $\alpha\text{-CH}_2$ main peaks at $\delta 2.77$ and $\delta 2.54$; the difference between the two peaks is 0.23 ppm.

Among the four pentads shown in Chart 2, the HT-HT pentad seems to be preferentially formed. If the



main $\alpha\text{-CH}_2$ peak of PTz(R)Th at about δ 3.2 is assigned to the HT-unit and other peak(s) at higher magnetic fields to the HH-unit, similar to cases of previously reported P3RTh and P4RTz.^{1–5} Regioregularity of PTz(Non)Th is estimated to be higher than 90%. For the preferable formation of the HT-HT pentad, it is conceivable that a selective coupling initially takes place between the C(2)–Br bond of Tz(R)Br₂ (cf. Scheme 1) and Th(SnMe₃)₂, due to the inductive effect of nitrogen next to the Br,²¹ to yield a dimer which has a structure similar to that of the starting dimer shown in Scheme 4. The palladium-catalyzed polycondensation of the dimer will give the HT-type PTz(R)Th.

Another possible explanation for the regioselective polycondensation is that the HT-type PTz(R)Th is preferentially formed since this structure is favorable for the formation of the π -stacked structure by side chain crystallization, which will be discussed later. The selectivity may arise from energetically stable π -stacked crystalline HT-PTz(R)Th. In relation to this, Andersson and Inganäs^{22a} and Ueda^{22b} reported that certain regioselection took place in oxidative polymerization of 3-alkylthiophene with FeCl₃, especially at lower temperatures. For the special oxidative polymerization reported by Andersson and Inganäs, P3RTh with an HT (head-to-tail) content of $94 \pm 2\%$ ^{22a} was achieved. In addition, it was reported that polymerization of propylene giving crystalline stereoregular poly(propylene) proceeded at a much faster velocity than that giving amorphous stereoirregular poly(propylene), presumably due to the stabilization energy attained by forming the crystal in the stereoregular polymerization.²³ It was also reported that selective stacking of regioregular HT-P3RTh and HT-P3R'Th occurred to form a crystalline HT-P3RTh solid and a crystalline HT-P3R'Th solid separately, when the solvent was removed by evaporation from a solution containing both HT-P3RTh and HT-P3R'Th;^{5f} this also supported a strong tendency for the formation of energetically advantageous crystalline structures for the π -conjugated polymers.

It is not easy to determine which factor (the first one is high selective reactivity of the C(2)–Br bond in Tz(R)Br₂; the second one is stacking stabilization) mainly determines the regioselectivity. However, the latter stacking stabilization seems to contribute, at least partly, to the regioselective polycondensation. It may be difficult to explain the regioselectivity only based on the selective high reactivity of the C(2)–Br bond. The high reactivity of the C(2)–Br bond may also partly lead to formation of a trimer similar to Tz(Hep)ThTz(Hep) shown in Scheme 3; of course the two ends of the trimer formed from Tz(R)Br₂ are brominated. If this trimer participates in the polycondensation, the regioregularity will be decreased. If the dimer is selectively formed in the early stage and this is polymerized, the regioregularity is expected to be maintained through the polycondensation. However, the chloroform-soluble part of PTz(Non)Th (vide ante) with a smaller molecular weight gave a lower HT content of about 80%, compared with

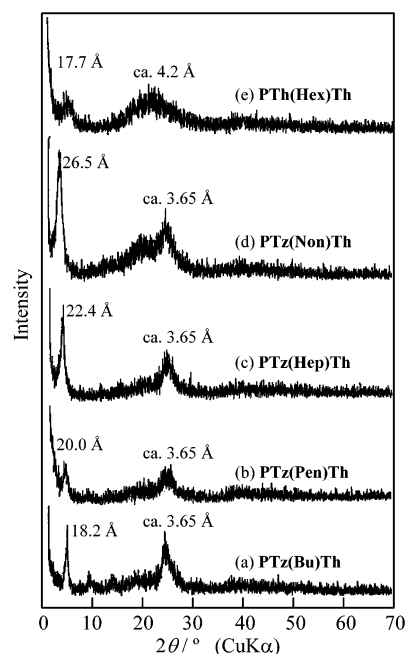


Figure 3. Powder XRD patterns of (a) PTz(Bu)Th, (b) PTz(Pen)Th, (c) PTz(Hep)Th, (d) PTz(Non)Th, and (e) PTh(Hex)Th.

that (higher than 90%) of whole PTz(Non)Th. Since the stacking of five-membered-ring π -conjugated polymers is enhanced with an increase in the molecular weight,^{5b} these data suggest the presence of the effect of the stacking on the regioselection. In relation to this, we carried out fractionation of two types of poly(3-hexylthiophene)s, P3HexTh's (P3HexTh(Fe) prepared by oxidative polymerization of 3-hexylthiophene with FeCl₃^{5b} and P3HexTh(Zn/Ni) prepared by Ni-catalyzed polycondensation of a zinc compound of 3-hexylthiophene^{2,5b}), according to their solubility in chloroform (good solvent),^{5b,g} methylene chloride, THF, hexane, and methanol (poor solvent)^{5b,g} and found that the regioregularity (the HT-content) of P3HexTh increased with an increase in the molecular weight of the fraction, as shown in the Supporting Information: e.g., from 81% at $M_n = 3000$ to 98% at $M_n = 33000$ for P3HexTh(Zn/Ni). These data also suggest the effect of stacking (or structural matching) on the regioregular polycondensation of five-membered-ring π -conjugated polymers, as in DNA, especially at high molecular weights.

Packing Structure in the Solid. Figure 3 exhibits powder XRD patterns of PTz(R)Th's; for comparison, that of the regiorandom PTh(Hex)Th prepared according to Scheme 2 is also shown. As shown in Figure 3, PTz(R)Th gives two main peaks: one with spacing d_1 in the low-angle region (2θ below 5°) and another at $d_2 = 3.65$ Å. On the other hand, regiorandom PTh(Hex)Th gives only a weak peak in the low-angle region and a broad peak at about $d = 4.2$ Å, the latter being characteristic of a side-to-side distance between alkyl chains.²⁴ Since the effective cross section of the alkyl chains is about $S = 20$ Å², their hexagonal-like aggregation gives $d = 4.2$ Å.

The distance of $d_2 = 3.65$ Å observed for PTz(R)Th is characteristic of π -stacked regioregular π -conjugated polymers;^{1–6} HT-P3RTh's and HH-P4RTz's give d_2 values of about 3.8 and 3.55–3.6 Å, respectively, the values being somewhat larger than the sheet-to-sheet distance of graphite (3.35 Å). On the other hand, the d_1

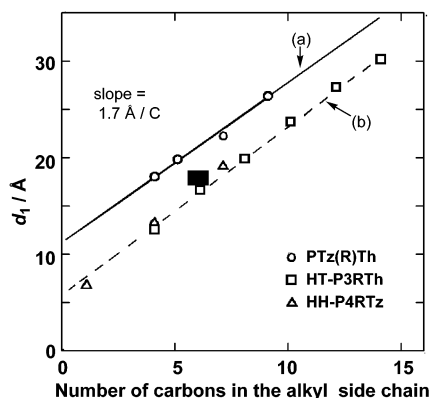
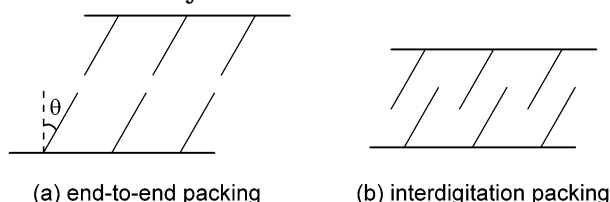


Figure 4. (a) Plots of d_1 spacing vs the number of carbons in the alkyl side chain of PTz(R)Th (○). For comparison, similar data for HT-P3RTh (□, line b), and HH-P4RTz (△) are given.

Chart 3. Two Packing Models for π -Conjugated Polymers with Side Chains



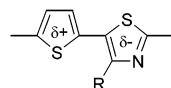
value of 18.2–26.5 Å calculated from the 2θ values of the diffraction peak in the low-angle region is usually assigned to the distance between main chains of the π -conjugated polymers separated by the alkyl side chains.^{1–6,25} The sharpness of the peak in the low-angle region is comparable to those observed with HT-P3RTh and HH-P4RTz.

Figure 4 indicates plots of the d_1 value versus the number of carbons in the alkyl side chain. For comparison, similar data for HT-P3RTh (□) and HH-P4RTz (△) are given in Figure 4.

As shown in Figure 4, the plots for PTz(R)Th give a straight line, and this straight line gives a slope of 1.7 Å/carbon, which is comparable to slopes obtained for HT-P3RTh (slope = 1.8 Å/carbon) and HH-P4RTz (2.0 Å/carbon).^{5b} Since one $-\text{CH}_2-$ group has a height of 1.25 Å/carbon,^{24–26} the obtained slope larger than 1.25 Å/carbon suggests that PTz(R)Th takes an end-to-end packing mode (Chart 3), similar to HT-P3RTh and HH-P4RTz.^{5b}

However, as seen in Figure 4, PTz(R)Th apparently gives larger d_1 -spacing than HT-P3RTh and HH-P4RTz. The intercept of the straight line (ca. 12 Å), which seems to correspond to the thickness of the π -conjugated main chain, is almost double the intercepts (ca. 6 Å) observed for HT-P3RTh (line b in Figure 4) and HH-P4RTz, as seen from Figure 4.

These results suggest the formation of a new end-to-end packing structure as shown in Figure 5. The XRD data support π -stacking of the end-to-end packed molecular sheet depicted in Figure 5. The CT structure between the electron-donating thiophene and electron-accepting thiazole unit seems to assist the formation of the packing structure. For the extended planar confor-



mation with standard dimensions, the height c of the

Chart 4. Two Possible Configurations of the Double Chain

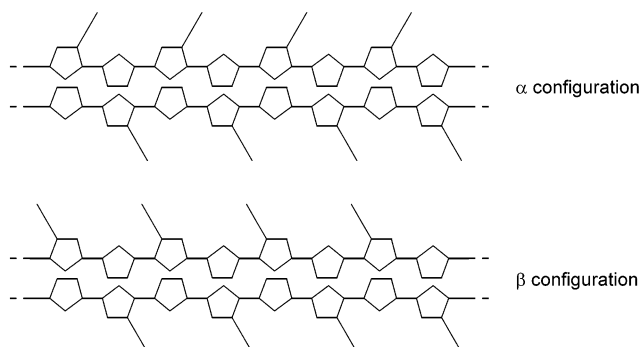
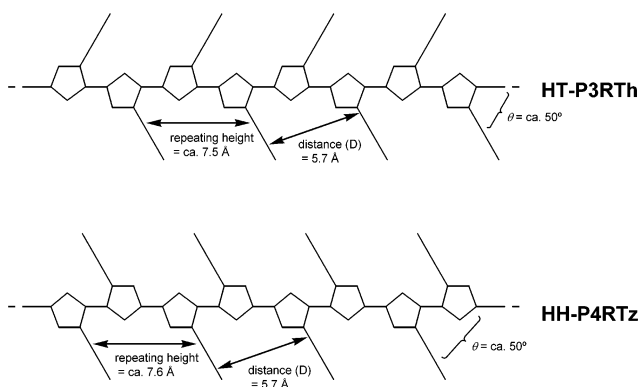


Chart 5. Structure of HT-P3RTh and HH-P4RTz^a



^a Reference 5b.

Th-Tz(R) unit along the polymer chain is estimated at 7.75 Å (cf. Figure 5). Therefore, the side area allotted to each alkyl side chain, area (A) = $cd_2 = 28 \text{ Å}^2$, is suited for the end-to-end packing in view of the effective cross section of the alkyl chain ($S = \text{ca. } 20 \text{ Å}^2$). If the polymer has straight alkyl side chains densely packed along the polymer chain, the slope of 1.7 Å/C corresponds to a tilt angle θ (cf. Chart 3) of about 45°, which is calculated to fit the following expected relation: $A (28 \text{ Å}^2) \approx S (20 \text{ Å}^2)/(\cos 45^\circ)$.

If PTz(R)Th has a highly regioregular structure, the double chain which is composed of A- and B-chains in Figure 5 will take either a parallel (α) or an antiparallel (β) configuration (Chart 4).

The α and β configurations correspond to the previously reported configurations of HT-P3RTh and HH-P4RTz, respectively, shown in Chart 5; ^{5b} both the polymers form the end-to-end packed and π -stacked structure in the solid. As seen in Chart 4, the α and β structures have a thicker thickness of the core main chain than HT-P3RTh and HH-P4RTz, corresponding to the larger intercept of the straight line in Figure 4 as discussed above.

When PTz(R)Th assumes the α configuration, it will form a π -stacked structure similar to the case of HT-P3RTh, and this packing model in the solid is depicted in the part a in Figure 6.

As discussed above, the sheet-to-sheet distance of $d_2 = 3.65 \text{ Å}$ calculated from the XRD peak is comparable to that (ca. 3.6 Å) observed with HH-P4RTz and somewhat shorter than that (ca. 3.8 Å) observed with HT-P3RTh. It was reported that the thiazole unit has a stronger tendency to form a face-to-face stacked structure than the thiophene unit.^{5d} The electrostatic interlayer attractive interaction between the thiophene

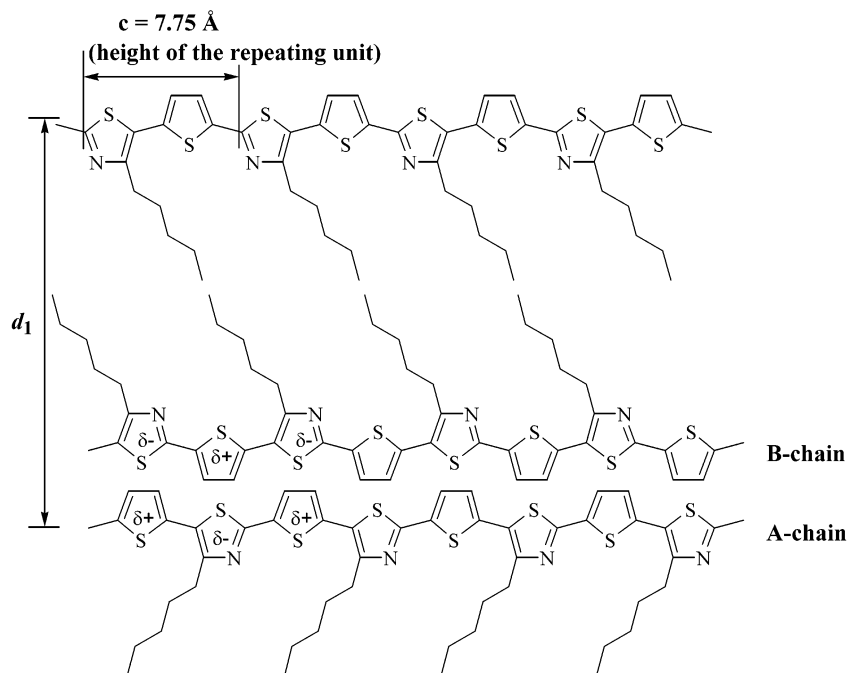


Figure 5. Packing model of PTz(R)Th in the solid. One sheet is shown. Below this sheet, another sheet comes.

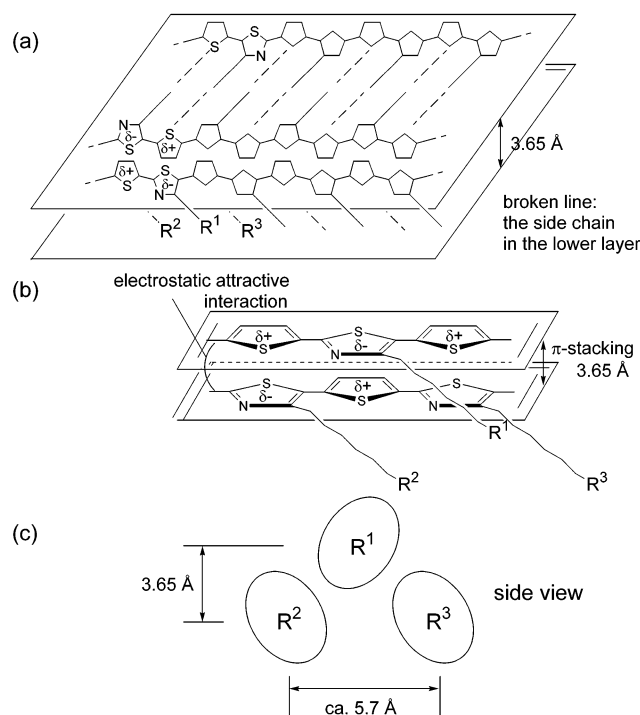


Figure 6. (a) Packing model for the α -configuration. This model is formed in a manner similar to that applied to construct the π -stacked structure of HT-P3RTh in the solid (refs 1–5). For the lower sheet, only the side R chains are shown by the broken lines for simplification. (b) A part of the stacked structure in part a is shown. (c) A side view of the R^1 – R^3 chains.

and thiazole units (cf. part b in Figure 6) will enhance the interlayer interaction to form a NaCl-like local structure. The β configuration in Chart 4, which corresponds to HH-P4RTz in Chart 5, will also form a similar stacked structure, because both HT-P3RTh and HH-P4RTz form analogous stacked structures.^{5b} Since HT-P3RTh and HH-P4RTz give analogous XRD patterns, it is difficult to determine whether PTz(R)Th forms the α or β configuration.

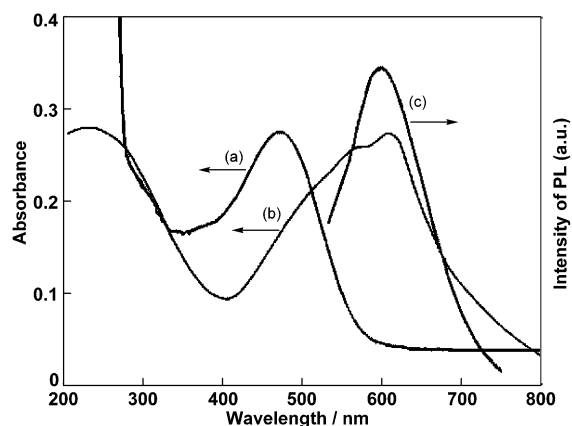


Figure 7. (a) UV-vis spectrum of PTz(Non)Th in CF_3COOH , (b) UV-vis spectrum of the film of PTz(Non)Th, and (c) PL spectrum of PTz(Non)Th in CF_3COOH . The cutoff wavelength of CF_3COOH is about 280 nm.

As described above, the axial height c (cf. Figure 5) of the repeating unit along the polymer chain is estimated at 7.75 Å. This packing model and the d_1 and d_2 values give calculated densities of 1.42, 1.38, 1.38, and 1.29 g cm^{-3} for PTz(Bu)Th, PTz(Pen)Th, PTz(Hep)Th, and PTz(Non)Th, respectively. These calculated densities essentially agree with the observed densities of 1.34, 1.36, 1.29, and 1.27 g cm^{-3} , supporting the packing structure, since polymers usually give a somewhat lower observed density due to containing amorphous parts.

Optical Data. As shown in Table 1, PTz(R)Th's give a UV-vis absorption peak at about 465 nm in CF_3COOH . For the cast film, the UV-vis absorption peak shifts to a longer wavelength. The UV-vis absorption band of the film has subpeaks characteristic of films of π -stacked polymers such as HT-P3RTh and HH-P4RTz,^{1–5} and the lowest transition energy peak appears at about 600 nm. Figure 7 exhibits the UV-vis spectrum of a CF_3COOH solution of PTz(Non)Th (curve a), the UV-vis spectrum of the cast film of PTz(Non)Th (curve b), and the photoluminescence (PL)

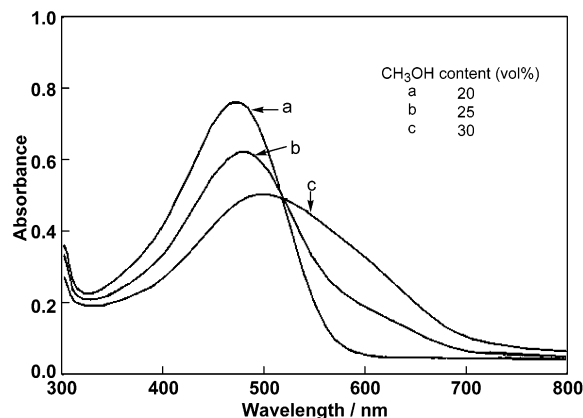


Figure 8. Changes of the UV-vis spectrum of PTz(Hep)Th with an increase in the fraction (vol/vol) of CH₃OH in a mixture of CH₃OH (poor solvent) and CF₃COOH (good solvent). CH₃OH was added to the CF₃COOH solution of PTz(Hep)Th. The concentration of PTz(Hep)Th was maintained constant (3.6×10^{-5} M of the repeating unit).

spectrum of the CF₃COOH solution of PTz(Non)Th (curve c). The PL peak appears near the onset position of the UV-vis absorption band as usually observed with π -conjugated compounds and polymers. The UV-vis absorption band of the film of PTz(Non)Th showed tailing toward the near-infrared region. This suggests that the UV-vis absorption band contains contributions from molecular assemblies with various degrees of assembly and the assembly with a higher order of assembling gives the UV-vis peak at a longer wavelength. Effects of the degree of molecular assembly on optical properties of π -conjugated polymers have been discussed.²⁷

It was reported that addition of a poor solvent (e.g., methanol) to a solution (e.g., CHCl₃ solution) of π -conjugated polymer causes formation of a colloidal solution which shows a bathochromic shift of the UV-vis peak approaching the UV-vis peak of the π -stacked solid when the π -conjugated polymer has a strong tendency to stack.^{5,28} PTz(R)Th showed similar optical changes when CH₃OH, a poor solvent for the polymer, was added to the CF₃COOH solution of the polymer. Figure 8 exhibits the example. These optical data support formation of the π -stacked solid and colloid of PTz(R)Th, similar to cases of HT-P3RTh and HH-P4RTz.

Conclusion

Organometallic polycondensation between the electron-donating thiophene and the electron-accepting alkyl thiazole gives a new CT-type π -conjugated polymer. ¹H NMR, XRD, and UV-vis data reveal that the polymer has a high regioregularity and a tendency to form a stacked structure. The regioregularity is considered to originate from a steric fitness of the polymer to form the precipitate and to be assisted by the CT structure of the polymer.

Acknowledgment. We are grateful to Professor T. Maruyama of our institute (now at The Yokohama Rubber Co. Ltd.) for helpful discussion. This research was partly supported by the 21 Century COE program. Thanks are due to Mr. Y. Sakai of Mitsubishi Chemical Corporation and Mr. K. Namekawa of our laboratory for experimental support.

Supporting Information Available: Regioregularity of fractionated poly(3-hexylthiophene). This material is available free of charge via the Internet at <http://pubs.acs.org>.

References and Notes

- (1) (a) McCullough, R. D.; Lowe, R. D. *J. Chem. Soc., Chem. Commun.* **1992**, 70. (b) McCullough, R. D.; Tristram-Nagle, S.; Williams, S. P.; Lowe, R. D.; Jayaraman, M. *J. Am. Chem. Soc.* **1993**, *115*, 4910. (c) McCullough, R. D.; Lowe, R. D.; Jayaraman, M.; Anderson, D. L. *J. Org. Chem.* **1993**, *58*, 904. (d) McCullough, R. D.; Ewband, P. C.; Loewe, R. S. *J. Am. Chem. Soc.* **1997**, *119*, 633. (e) McCullough, R. D. *Adv. Mater.* **1998**, *10*, 93.
- (2) (a) Chen, T.-A.; Rieke, R. D. *J. Am. Chem. Soc.* **1992**, *114*, 10087. (b) Chen, T.-A.; Rieke, R. D. *Synth. Met.* **1993**, *60*, 175. (c) Wu, X.; Chen, T.-A.; Rieke, R. D. *Macromolecules* **1995**, *28*, 2101. (d) Chen, T.-A.; Wu, X.; Rieke, R. D. *J. Am. Chem. Soc.* **1995**, *117*, 233.
- (3) (a) Miller, L. L.; Mann, K. R. *Acc. Chem. Res.* **1996**, *29*, 417. (b) Graf, D. D.; Duan, R. G.; Campbell, J. P.; Miller, L. L.; Mann, K. R. *J. Am. Chem. Soc.* **1997**, *119*, 5888.
- (4) (a) Märdalen, J.; Samuelsen, E.; Gautun, O. R.; Carlsen, P. H. *Solid State Commun.* **1991**, *80*, 687. (b) Winokur, M. J.; Wamsley, P.; Moulton, J.; Smith, P.; Heeger, A. J. *Macromolecules* **1991**, *24*, 3812. (c) Watanabe, J.; Harkness, B. R.; Sone, M.; Ichimura, H. *Macromolecules* **1994**, *27*, 507.
- (5) (a) Yamamoto, T. *Chem. Lett.* **1996**, 703. (b) Yamamoto, T.; Komarudin, D.; Arai, M.; Lee, B.-L.; Suganuma, H.; Asakawa, N.; Inoue, Y.; Kubota, K.; Sasaki, S.; Fukuda, T.; Matsuda, H. *J. Am. Chem. Soc.* **1998**, *120*, 2047. (c) Yamamoto, T.; Suganuma, H.; Maruyama, T.; Inoue, T.; Muramatsu, Y.; Arai, M.; Komarudin, D.; Ooba, N.; Tomaru, S.; Sasaki, S.; Kubota, K. *Chem. Mater.* **1997**, *9*, 1217. (d) Yamamoto, T.; Lee, B.-L.; Suganuma, H.; Sasaki, S. *Polym. J.* **1998**, *30*, 853. (e) Yamamoto, T.; Suganuma, H.; Maruyama, T.; Kubota, K. *J. Chem. Soc., Chem. Commun.* **1995**, 1613. (f) Yamamoto, T.; Kokubo, H. *J. Polym. Sci., Part B: Polym. Phys.* **2000**, *38*, 84. (g) Yamamoto, T.; Oguro, D. *Macromolecules* **1996**, *29*, 1833.
- (6) (a) Yamamoto, T.; Kokubo, H.; Morikita, T. *J. Polym. Sci., Part B: Polym. Phys.* **2001**, *39*, 1713. (b) Morikita, T.; Yamaguchi, I.; Yamamoto, T. *Adv. Mater.* **2001**, *13*, 1862. (c) Yamamoto, T.; Shiraishi, K.; Mahmut, A.; Yamaguchi, I.; Groenendaal, L. B. *Polymer* **2002**, *43*, 2993. (d) Yamamoto, T.; Lee, B.-L. *Macromolecules* **2002**, *35*, 2993.
- (7) (a) Nanos, J. I.; Kampf, J. W.; Curtis, M. D.; Gonzalez, L.; Martin, D. C. *Chem. Mater.* **1995**, *7*, 2332. (b) Politis, J. K.; Nemes, J. C.; Curtis, M. D. *J. Am. Chem. Soc.* **2001**, *123*, 2537.
- (8) (a) Banguy, C. G.; Evans, U.; Myrick, M. L.; Bunz, U. H. F. *Macromolecules* **2001**, *34*, 7592. (b) Perahia, D.; Traiphon, R.; Bunz, U. H. F. *J. Chem. Phys.* **2002**, *117*, 1827. (c) Bunz, U. H. F.; Enkelmann, V.; Kloppenburg, L.; Jones, D.; Shimizu, K. D.; Claridge, J. B.; zur Loye, H.-C.; Lieser, G. *Chem. Mater.* **1999**, *11*, 1416.
- (9) (a) Siringhaus, H.; Brown, P. J.; Friend, R. H.; Nielsen, M. M.; Bechgaard, K.; Langeveld-Boss, B. M. W.; Spiering, J. H.; Janssen, R. A. J.; Meijer, E. W.; Herwig, P.; de Leeuw, D. M. *Nature* **1999**, *401*, 685. (b) Sherf, U.; List, E. J. W. *Adv. Mater.* **2002**, *14*, 477.
- (10) When the π -conjugated polymer has spacing groups such as $-\text{CH}=\text{CH}-$ and $-\text{C}\equiv\text{C}-$ groups, polymers consisting of six-membered rings (e.g., $-(\text{benzothiazole-4,7-diyl}-\text{C}\equiv\text{C}-2,5\text{-dialkoxybenzene-1,4-diyl})_n-$) (refs 6a,b and 8) can form the stacked structure.
- (11) (a) Zhou, Z.-H.; Maruyama, T.; Kanbara, T.; Ikeda, T.; Ichimura, K.; Yamamoto, T.; Tokuda, K. *J. Chem. Soc., Chem. Commun.* **1991**, 1210. (b) Yamamoto, T.; Zhou, Z.-H.; Kanbara, T.; Shimura, M.; Kizu, K.; Maruyama, T.; Nakamura, Y.; Fukuda, T.; Lee, B.-L.; Ooba, N.; Tomaru, S.; Kurihara, T.; Kaino, T.; Kubota, K.; Sasaki, S. *J. Am. Chem. Soc.* **1996**, *118*, 10389. (c) Lee, B.-L.; Yamamoto, T. *Macromolecules* **1999**, *32*, 1375.
- (12) (a) Ferraris, J. P.; Bravo, A.; Kim, W.; Hrnir, D. C. *J. Chem. Soc., Chem. Commun.* **1994**, 991. (b) Karikomi, M.; Kitamura, C.; Tanaka, S.; Yamashita, Y. *J. Am. Chem. Soc.* **1995**, *117*, 6791.
- (13) (a) Zhu, S. S.; Swager, T. M. *Adv. Mater.* **1996**, *8*, 497. (b) van Müllekom, H. A. M.; Vekemans, J. A. J. M.; Meijer, E. W. *Chem. Commun.* **1996**, 2163.

- (14) (a) Zhang, Q. T.; Tour, J. M. *J. Am. Chem. Soc.* **1997**, *119*, 5065. (b) Zhang, Q. T.; Tour, J. M. *J. Am. Chem. Soc.* **1998**, *120*, 5355.
- (15) (a) Havinga, E. E.; Ten Hoeve, W.; Wynberg, H. *Polym. Bull. (Berlin)* **1992**, *29*, 119. (b) Eldo, J.; Ajayaghosh, A. *Chem. Mater.* **2002**, *14*, 410.
- (16) Doyle, M. P.; Siegfried, B.; Dellaria, J. F., Jr. *J. Org. Chem.* **1977**, *42*, 2425.
- (17) Coulson, D. *Inorg. Synth.* **1972**, *13*, 121.
- (18) π -Conjugated polymers with imine nitrogen sometimes have interaction with GPC columns, which will give estimated M_n and M_w that are lower than the real values.
- (19) (a) Aizawa, M.; Watanabe, S.; Shinohara, H.; Shirakawa, H. *Denki Kagaku* **1984**, *52*, 81. (b) Yamamoto, T.; Sanechika, K.; Yamamoto, A. *J. Polym. Sci., Polym. Lett. Ed.* **1980**, *18*, 9. (c) Kobayashi, M.; Chen, J.; Chung, T.-C.; Moraes, F.; Heeger, A. J.; Wudl, F. *Synth. Met.* **1984**, *9*, 77. (d) Yamamoto, T.; Kanbara, T.; Mori, C.; Wakayama, H.; Fukuda, T.; Inoue, T.; Sasaki, S. *J. Phys. Chem.* **1996**, *100*, 12631.
- (20) (a) Lère-Porte, J.-P.; Moreau, J. J.; Torreillers, C. *Eur. J. Org. Chem.* **2001**, 1249. (b) Yamamoto, T.; Honda, Y.; Kokubo, H. *Polymer*, submitted.
- (21) Marsella, M. J.; Fu, D.-K.; Swager, T. M. *Adv. Mater.* **1995**, *7*, 145.
- (22) (a) Andersson, M. R.; Selse, D.; Berggren, M.; Järvinen, H.; Hjerberg, T.; Inganäs, O.; Wennerström, O.; Österholm, J. E. *Macromolecules* **1994**, *27*, 6503. (b) Amou, S.; Hoba, O.; Shirato, K.; Hayakawa, T.; Ueda, M.; Takeuchi, K.; Asai, M. *J. Polym. Sci., Part A: Polym. Chem.* **1999**, *37*, 1943.
- (23) Soga, K.; Ohgisawa, M.; Shiono, T. *Makromol. Chem. Rapid Commun.* **1989**, *10*, 503.
- (24) (a) Jordan, E. F., Jr.; Feideisen, D. W.; Wrigley, A. N. *J. Polym. Sci., Part A-1* **1971**, *9*, 1835. (b) Hsieh, H. W.; Post, B.; Morawetz, H. *J. Polym. Sci., Polym. Phys. Ed.* **1976**, *14*, 1241. (c) Swan, P. R. *J. Polym. Sci.* **1962**, *56*, 403.
- (25) (a) Yamamoto, T. *Macromol. Rapid Commun.* **2002**, *23*, 583. (b) Yamamoto, T. *Synlett* **2003**, 425.
- (26) Piesczek, Y.; Strobl, G. R.; Malzahn, K. *Acta Crystallogr.* **1974**, *B30*, 1278.
- (27) (a) *Handbook of Organic Conductive Molecules and Polymers*; Nalwa, H. S., Ed.; John Wiley: Chichester, 1997. (b) Yamamoto, T.; Lee, B.-L. *Macromolecules* **2002**, *35*, 2993.
- (28) (a) Inganäs, O.; Salaneck, W. R.; Österholm, J.-E.; Laakso, J. *Synth. Met.* **1988**, *22*, 395. (b) Sandstedt, C. A.; Rieke, R. D.; Eckhardt, C. J. *Chem. Mater.* **1995**, *7*, 1057. (c) Faid, K.; Frechette, M.; Ranger, M.; Mazerolle, L.; Levesgue, I.; Leclerc, M.; Chen, T. A.; Rieke, R. D. *Chem. Mater.* **1995**, *7*, 1390. (d) Kokubo, H.; Yamamoto, T. *Macromol. Chem. Phys.* **2001**, *202*, 1031.

MA030167N